

Static and Microwave Properties of Amorphous Magnets Near Saturation

Eugene M. Chudnovsky and Dmitry A. Garanin

*Physics Department, Herbert H. Lehman College and Graduate School, The City University of New York,
250 Bedford Park Boulevard West, Bronx, New York 10468-1589, USA*

(Dated: October 30, 2024)

Static and dynamic properties of magnetically soft amorphous ferromagnets have been studied analytically and numerically within random-field and random-anisotropy models. External field and coherent anisotropy that are weak compared to their random counterparts are sufficient to bring the magnet close to saturation. The scaling of spin-spin correlations in this regime is computed, and its dependence on parameters is confirmed by Monte Carlo simulation. We show that near the ferromagnetic resonance, the spin excitations are damped and spatially localized due to randomness even close to saturation. On increasing the strength of randomness, the localization length goes down in accordance with theoretical expectations, while the damping of spin excitations goes up.

I. INTRODUCTION

Static properties of amorphous magnets have been studied theoretically within the random field (RF) and random anisotropy (RA) models [1–15] since the early 1980s. Both models assume a ferromagnetic exchange between neighboring spins and a random field or random magnetic anisotropy acting on each spin. The behavior of the magnetization in an amorphous magnet is illustrated by Fig. 1. It was first understood by Imry and Ma [16] for arbitrary systems with a continuous order parameter and quenched randomness. In application to disordered magnets, it comes from the competition between random local forces rotating the spins and the ferromagnetic exchange that favors their uniform alignment. This competition results in a finite ferromagnetic correlation length that increases on decreasing the strength of the local disordering forces.

Theoretical work on the dynamical properties of the RF and RA models has been scarce, mainly focused [17] on the phenomenology of the ferromagnetic resonance (FMR) investigated experimentally [18–23]. In accordance with general theoretical arguments [24–35], localization of spin modes was observed in experiments on disordered magnets [36–42]. More recently, localized spin-wave excitations generated by microwaves in the RA system have been studied on large spin lattices numerically [43, 44]. It was demonstrated [43–48] that random-anisotropy magnets can be promising materials for broadband microwave absorption. This material property is pursued due to its numerous technological applications such as, e.g., microwave shielding, thermal cancer treatment, and stealth technology [49]. Nanoscale inhomogeneity of the magnetization in amorphous random-anisotropy magnets [50, 51], see Fig. 1, resembles nanocomposites [52, 53] with embedded magnetic particles but has an advantage of a greater magnetic volume available for microwave absorption.

In this paper, we study within microscopic models the static and dynamic properties of RF and RA magnets close to saturation caused by either the external magnetic field or coherent (global) magnetic anisotropy. The importance of this problem becomes clear from the mag-

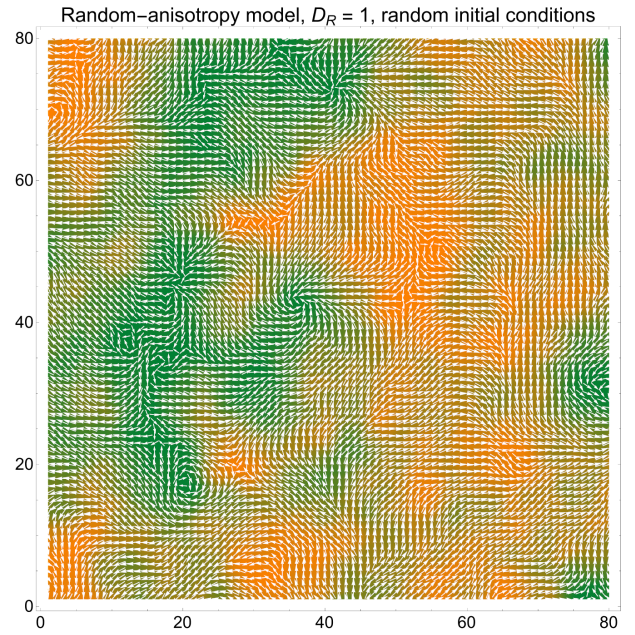


Figure 1. Equilibrium spin structure in a 2D RA model for $D_R/J = 1$ and $T = 0$ obtained numerically by the energy minimization starting from a random initial condition. In-plane spin components are shown by white arrows. The out-of-plane component is shown by orange/green corresponding to positive/negative. Axes labels are distances in lattice units.

netic softness of such magnets. As we shall see, a magnetic field that is weak compared to the RF, or the coherent anisotropy (CA) that is weak compared to the RA, is sufficient to bring the magnet close to saturation. Some CA would inevitably be present in an amorphous magnet due to the manufacturing process. Thus the static and dynamic properties of the CA+RA model, including microwave absorption, require special consideration, as compared to the pure RA model [43–48].

The characteristic scale of the spatial fluctuations of the magnetization is the ferromagnetic correlation length. In RF and RA models it corresponds to the average size of Imry-Ma domains due to randomness illustrated by Fig. 1. When it is small compared to the size of con-

ventional magnetic domains originating from magnetic dipolar forces, or when the size of the system is small compared to the typical size of such domains, the magnetic dipole-dipole interaction between the spins can be neglected. Here we consider such a situation.

Both problems, RF and RA, are highly nonlinear. However, the RF problem is easier to tackle analytically. While it is more theoretical than practical, it serves as a precursor for the RA problem. For a weak RF it allows one to obtain rigorous scaling of physical quantities with parameters. Then, using the IM argument, and the language of the anisotropy field, that scaling can be translated into the dependence of the physical quantities on the CA+RA model on the parameters. The latter can be tested in a numerical experiment, which will be done here.

The paper is organized as follows. Static spin-spin correlations are studied for the three-component spins in three (bulk solid) and two (thin film) dimensions in Section II. This is done analytically within the RF model, first without an external field, Section II A, and then analytically in the presence of the external field, Section II B. The obtained scaling is extended to the dependence of static spin-spin correlations on parameters in the CA+RA model, which is confirmed numerically in Section II C. Dynamical properties close to saturation are studied in Section III. First, the analytical theory of spin excitations in the RF model with the external field is presented in Section III A. Then excitations in the CA+RA model are studied numerically in Section III B and their localization length is computed. Section III C illustrates the dynamics of the system in the presence of RA that causes damping of the uniform precession. Our conclusions are outlined in Section IV.

II. FERROMAGNET WITH WEAK STATIC RANDOMNESS CLOSE TO SATURATION

We shall consider two models, the random-field (RF) model with the Hamiltonian

$$\mathcal{H} = -\frac{1}{2} \sum_{ij} J_{ij} \mathbf{s}_i \cdot \mathbf{s}_j - \sum_i \mathbf{h}_i \cdot \mathbf{s}_i - \mathbf{H} \cdot \sum_i \mathbf{s}_i, \quad (1)$$

and the random anisotropy (RA) model with the Hamiltonian

$$\mathcal{H} = -\frac{J}{2} \sum_{ij} \mathbf{s}_i \cdot \mathbf{s}_j - \frac{D_R}{2} \sum_i (\mathbf{n}_i \cdot \mathbf{s}_i)^2 - \frac{D_C}{2} \sum_i (\mathbf{n}_c \cdot \mathbf{s}_i)^2, \quad (2)$$

Here \mathbf{s}_i is a n -component constant-length ($|\mathbf{s}_i| = s$) spin at the site i of a cubic lattice. The summation is over the nearest neighbors. In Eq. (1) \mathbf{h}_i is a static random field at a site i , while in Eq. (2) \mathbf{n}_i represents the direction of random magnetic anisotropy at a site i , with D_R being its strength. In the first equation \mathbf{H} is the external magnetic field, while in the second equation D_C is the

strength of the coherent magnetic anisotropy having the same direction \mathbf{n}_c at each lattice site.

While these two models are mathematically different, they are conceptually similar. Both RF and RA satisfying the condition $h, D_R \ll J$ slightly perturb directions of the spins away from the parallel alignment that is preferred by the strong ferromagnetic exchange, while both the external magnetic field and the coherent anisotropy (CA) provide the preferred direction of the global magnetization. The RF model is easier to treat analytically, which we will do first. The scaling of physical parameters on h/J and H/J will be established. Then the RA model will be studied numerically and its equivalence to the RF model in terms of the scaling on D_R/J and D_C/J will be confirmed.

A. Spin correlations in the RF model at $\mathbf{H} = 0$: Analytical theory

The continuous counterpart of the RF model, Eq. (1), is described by the Hamiltonian

$$\mathcal{H} = \int d^d r \left[\frac{\alpha}{2} (\nabla \mathbf{S})^2 - \mathbf{h} \cdot \mathbf{S} - \mathbf{H} \cdot \mathbf{S} \right]. \quad (3)$$

Here \mathbf{S} is a spin field of constant length $S = s/a^d$ in d spatial dimensions and $\alpha = Ja^{d+2}$ is the exchange stiffness, with a being the lattice spacing. We use uncorrelated RF satisfying

$$\langle h_{i\alpha} h_{j\beta} \rangle = \frac{h^2}{n} \delta_{\alpha\beta} \delta_{ij}, \quad (4)$$

for the lattice model and

$$\langle h_\alpha(\mathbf{r}') h_\beta(\mathbf{r}'') \rangle = \frac{h^2}{n} \delta_{\alpha\beta} a^3 \delta(\mathbf{r}' - \mathbf{r}'') \quad (5)$$

for the continuous model, with Greek indices being the Cartesian components of the vectors and $|\mathbf{h}_i| = h = \text{const}$. Within this model, one obtains in 3D in the absence of the external field [12]

$$\frac{1}{2S^2} \langle [\mathbf{S}(\mathbf{r}_1) - \mathbf{S}(\mathbf{r}_2)]^2 \rangle = \frac{|\mathbf{r}_1 - \mathbf{r}_2|}{R_f} \quad (6)$$

for $|\mathbf{r}_1 - \mathbf{r}_2| \ll R_f$ with

$$\frac{R_f}{a} = \frac{8\pi\alpha_e^2 S^2}{h^2 a^4 (1 - 1/n)} = \frac{8\pi}{(1 - 1/n)} \left(\frac{Js}{h} \right)^2. \quad (7)$$

Noticing that

$$\frac{1}{2S^2} \langle [\mathbf{S}(\mathbf{r}_1) - \mathbf{S}(\mathbf{r}_2)]^2 \rangle = 1 - \frac{1}{S^2} \langle \mathbf{S}(\mathbf{r}_1) \cdot \mathbf{S}(\mathbf{r}_2) \rangle \quad (8)$$

this gives

$$\langle \mathbf{s}_i \cdot \mathbf{s}_j \rangle = s^2 \left(1 - \frac{|\mathbf{r}_i - \mathbf{r}_j|}{R_f} \right). \quad (9)$$

Based upon this result, and assuming that spin-spin correlations in the RF model at $H = 0$ decay exponentially (as suggested by the IM argument and confirmed by the numerical analysis [11]) one can use

$$\langle \mathbf{s}_i \cdot \mathbf{s}_j \rangle = s^2 \exp\left(-\frac{|\mathbf{r}_i - \mathbf{r}_j|}{R_f}\right) \quad (10)$$

as a good approximation for arbitrary $|\mathbf{r}_i - \mathbf{r}_j|$. Similar consideration in 2D gives $R_f/s \propto Js/h$.

B. Spin correlations in the RF model near saturation: Analytical theory

We shall now turn to the RF model with a nonzero external field $\mathbf{H} = H\hat{z}$. To account for the constant length of the spin field, we consider the Hamiltonian

$$\mathcal{H}_\lambda = \int d^d r \left[\frac{\alpha}{2} (\nabla \mathbf{S})^2 - \mathbf{h} \cdot \mathbf{S} - \mathbf{H} \cdot \mathbf{S} - \lambda(\mathbf{r}) \mathbf{S}^2 \right] \quad (11)$$

with the Lagrange multiplier $\lambda(\mathbf{r})$. Properties of this model near saturation have been previously studied for XY spins in three dimensions[10]. We shall now extend this study to the three-component spins in three and two dimensions.

The extremal field $\mathbf{S}(\mathbf{r})$ corresponding to the Hamiltonian (11) satisfy

$$\alpha_e \nabla^2 \mathbf{S} + \mathbf{H} + \mathbf{h} + 2\lambda \mathbf{S} = 0. \quad (12)$$

with λ provided by the condition $\mathbf{S}^2 = S^2$:

$$\lambda = -\frac{1}{2S^2} (\alpha_e \mathbf{S} \cdot \nabla^2 \mathbf{S} + \mathbf{S} \cdot \mathbf{H} + \mathbf{S} \cdot \mathbf{h}) \quad (13)$$

This gives

$$\nabla^2 \mathbf{S} - \frac{1}{S^2} (\mathbf{S} \cdot \nabla^2 \mathbf{S}) \mathbf{S} - \frac{1}{\alpha_e S^2} (\mathbf{S} \cdot \mathbf{H} + \mathbf{S} \cdot \mathbf{h}) \mathbf{S} = -\frac{1}{\alpha_e} (\mathbf{H} + \mathbf{h}). \quad (14)$$

Close to the saturation, one can write

$$\mathbf{S} = \mathbf{S}_0(\mathbf{r}) = S\hat{z} + s_z \hat{z} + \mathbf{s}_\perp \quad \text{with} \quad |s_\perp|, |s_\parallel| \ll S. \quad (15)$$

Here $s_z \hat{z}$ and \mathbf{s}_\perp are oscillating (in space) components of the spin field due to the random field. Linearization of the above equation then gives

$$\begin{aligned} \nabla^2 s_z \hat{z} + \nabla^2 \mathbf{s}_\perp - \nabla^2 s_z \hat{z} - \frac{1}{\alpha_e S} H s_z \hat{z} - \frac{1}{\alpha_e} h_z \hat{z} \\ - \frac{1}{\alpha_e S} H s_z \hat{z} - \frac{1}{\alpha_e S} H \mathbf{s}_\perp = -\frac{1}{\alpha_e} h_z \hat{z} - \frac{1}{\alpha_e} \mathbf{h}_\perp, \end{aligned} \quad (16)$$

which implies $s_z = 0$ in the first order on \mathbf{h} while \mathbf{s}_\perp satisfies

$$(\nabla^2 - k_H^2) \mathbf{s}_\perp = -\frac{1}{J a^{d+2}} \mathbf{h}_\perp \quad (17)$$

where

$$k_H^2 \equiv \frac{H}{J S a^{d+2}} = \frac{H}{J s a^2}, \quad \frac{1}{k_H} = R_H = a \sqrt{\frac{J s}{H}}. \quad (18)$$

Here we have used the relations $\alpha_e = J a^{d+2}$, $S = s/a^d$.

The length R_H represents the correlation length describing the wandering of the transverse component of the magnetization. The close-to-saturation condition is equivalent to $a \ll R_H \ll R_f$, where R_f is the ferromagnetic correlation length at $H = 0$. Since R_H scales as $(Js/H)^{1/2}$, while R_f scales as $(Js/h)^2$ in 3D and as Js/h in 2D, this condition shows that the external field that is very weak compared to the random field may be sufficient to saturate the system. This agrees with a well-known experimental fact that RF (RA) magnets are magnetically very soft. It also shows that the regime close to saturation covers almost the entire range of the magnetic field that would be available in the experiment.

Implicit solution of Eq. (17) is

$$\mathbf{s}_\perp(\mathbf{r}) = -\frac{1}{J a^{d+2}} \int d^d r' G(\mathbf{r} - \mathbf{r}') \mathbf{h}_\perp(\mathbf{r}'). \quad (19)$$

where $G(r)$ is the Green function of Eq. (17), $G(r) = -e^{-k_H r}/(4\pi r)$ in 3D and $G(r) = K_0(k_H r)/(2\pi)$ in 2D, with K_0 being the Macdonald function. This gives

$$\begin{aligned} \langle \mathbf{s}_\perp(\mathbf{r}_1) \cdot \mathbf{s}_\perp(\mathbf{r}_2) \rangle &= \frac{1}{J^2 a^{2d+4}} \int d^d r' \int d^d r'' \times \\ &G(\mathbf{r}_1 - \mathbf{r}') G(\mathbf{r}_2 - \mathbf{r}') (\mathbf{h}_\perp(\mathbf{r}') \cdot \mathbf{h}_\perp(\mathbf{r}'')). \end{aligned} \quad (20)$$

Substituting here

$$\langle \mathbf{h}_\perp(\mathbf{r}') \cdot \mathbf{h}_\perp(\mathbf{r}'') \rangle = \frac{2}{3} h^2 a^d \delta(\mathbf{r}' - \mathbf{r}''). \quad (21)$$

we obtain

$$\langle \mathbf{s}_\perp(\mathbf{r}_1) \cdot \mathbf{s}_\perp(\mathbf{r}_2) \rangle = \frac{2h^2}{3J^2 a^{d+4}} \int d^d r G(\mathbf{r}_1 - \mathbf{r}) G(\mathbf{r}_2 - \mathbf{r}). \quad (22)$$

In 3D it gives

$$\langle \mathbf{s}_\perp(\mathbf{r}_1) \cdot \mathbf{s}_\perp(\mathbf{r}_2) \rangle = \frac{h^2}{12\pi J^2 a^7 k_H} e^{-k_H |\mathbf{r}_1 - \mathbf{r}_2|}. \quad (23)$$

The magnitude of the fluctuations of \mathbf{s}_\perp is provided by this expression at $\mathbf{r}_1 = \mathbf{r}_2$,

$$\langle s_\perp^2 \rangle = \frac{h^2}{12\pi J^2 a^7 k_H} = \left(\frac{2R_H}{3R_f} \right) S^2 \ll S^2. \quad (24)$$

On the approach to saturation, in the field range satisfying $a \ll R_H \ll R_f$, one has

$$S_z = S - \frac{1}{2S} \langle s_\perp^2 \rangle \quad (25)$$

$$1 - \frac{S_z}{S} = \frac{h^2}{24\pi J^2 S^2 a^7 k_H} = \frac{1}{24\pi} \left(\frac{h}{J s} \right)^2 \sqrt{\frac{J s}{H}}. \quad (26)$$

At very high fields, when R_H becomes formally smaller than a , the magnetization law on the approach to saturation changes. In this case the Laplacian in Eq (17) becomes irrelevant and one has

$$\mathbf{s}_\perp = \frac{\mathbf{h}_\perp}{Ja^{d+2}k_H^2} = \frac{\mathbf{h}_\perp}{H}S, \quad \langle \mathbf{s}_\perp^2 \rangle = \frac{\langle \mathbf{h}_\perp^2 \rangle}{H^2}S^2, \quad (27)$$

so that

$$1 - \frac{S_z}{S} = \frac{1}{3} \left(\frac{h}{H} \right)^2. \quad (28)$$

In 2D one has

$$\langle \mathbf{s}_\perp(\mathbf{r}_1) \cdot \mathbf{s}_\perp(\mathbf{r}_2) \rangle = \frac{h^2}{6\pi J^2 a^6 k_H^2} |\mathbf{r}_1 - \mathbf{r}_2| K_1(k_H |\mathbf{r}_1 - \mathbf{r}_2|). \quad (29)$$

Noticing that $K_1(x) \rightarrow [\pi/(2x)]^{1/2} \exp(-x)$ at large x and $K_1(x) \rightarrow 1/x$ at $x \rightarrow 0$, we obtain the magnitude of the fluctuations of \mathbf{s}_\perp in 2D:

$$\langle \mathbf{s}_\perp^2 \rangle = \frac{h^2}{6\pi J^2 a^6 k_H^2} \sim \left(\frac{R_H}{R_f} \right)^2 S^2 \ll S^2. \quad (30)$$

Consequently in 2D one must have in the field range satisfying $a \ll R_H \ll R_f$

$$1 - \frac{S_z}{S} = \frac{h^2}{12\pi J^2 S^2 a^6 k_H^2} = \frac{1}{12\pi} \left(\frac{h}{Js} \right)^2 \left(\frac{Js}{H} \right) \quad (31)$$

on the approach to saturation. At very high fields, the approach to saturation in 2D is given by the same law, Eq. (28), as in 3D.

Notice that in all dimensions the crossover to the high-field regime, $1 - S_z/S = (1/3)(h/H)^2$, occurs at the exchange field $H \sim 4\pi Js$. Such a field would hardly be available in amorphous ferromagnets with an atomic disorder. However in disordered ferromagnets with large amorphous structure factor or sintered ferromagnets with $R_a \gg a$, the effective exchange interaction per spin of the grain becomes $J(a/R_a)^2$. Consequently, the corresponding effective exchange field, $H \sim 4\pi Js(a/R_a)^2$, at which the crossover occurs from the $1/\sqrt{H}$ regime in 3D or $1/H$ in 2D to the $1/H^2$ high-field regime on approach to saturation would be within experimental reach.

C. Spin correlations in the RA model with coherent anisotropy: Numerical experiment

The RA model has a greater nonlinearity than the RF model and is more difficult to treat by analytical methods. However, as has been already mentioned, the two models are similar when described in terms of the Imry-Ma argument. This is reflected in the concept of the anisotropy field that is commonly used in magnetism. In the RA model, one should therefore expect that the ratios h/J and H/J that determine the behavior of physical

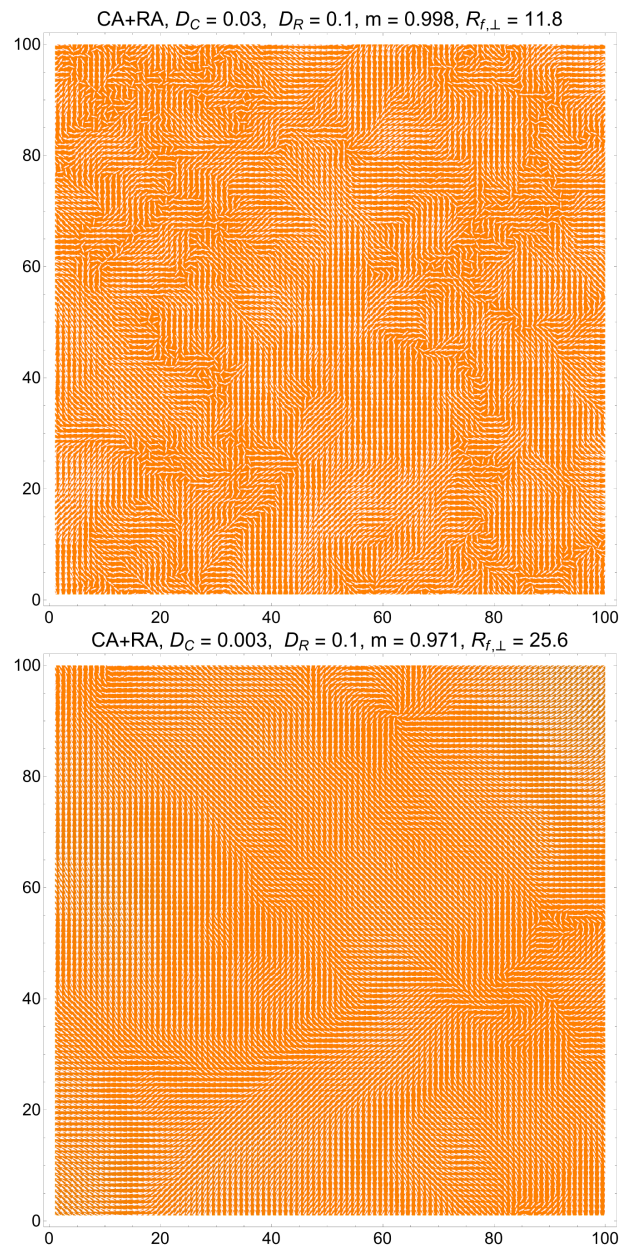


Figure 2. Transverse spin components (white arrows) in a 2D RA model in the presence of coherent anisotropy. The transversal correlation length increases as the coherent anisotropy decreases from $D_C/J = 0.03$ (upper panel) to $D_C/J = 0.003$ (lower panel).

quantities in the RF model will be replaced by the ratios D_R/J and D_C/J in the RA model.

We prepare the states of the CA+RA system at $T = 0$ by the energy minimization starting from the collinear spin state along z axis and in these states, we extract the values of the transverse ferromagnetic correlation radius $R_{f,\perp}$ from the values of the transverse magnetization components, $m_x^2 + m_y^2$ assuming a Gaussian shape of the magnetic correlation functions. Our numerical method has been described in detail in Refs. 43–45, and 47. It

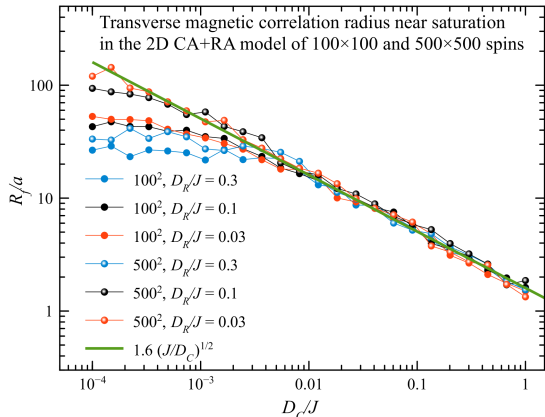


Figure 3. Dependence of the transversal correlation length $R_{f,\perp}$ on coherent anisotropy D_C in a 2D RA model. It follows theoretical prediction $R_{f,\perp} \propto (J/D_C)^{1/2}$ as soon as $R_{f,\perp}$ becomes small compared to the linear size of the system.

reproduces the analytical results of the RF model. To avoid redundancy, here we will only present the numerical results for the CA+RA model. In Fig. 2 we show the transverse components of the magnetization in the CA+RA model close to saturation. Weak CA has been chosen, $D_C/J = 0.03$ (upper panel) and $D_C/J = 0.003$ (lower panel) compared to the RA with $D_R/J = 0.1$. In both cases the system is close to saturation, 99.8% for $D_C/J = 0.03$ and 97.1% for $D_C/J = 0.003$. This is in accordance with the expectation based upon the results of the previous section that $D_C \ll D_R$ is sufficient to almost saturate the system. Slightly lower magnetization for weaker CA is expected from the fact that the ordering due to the CA competes with the disordering due to the RA.

Fig. 3 shows the dependence of the transversal correlation length, $R_{f,\perp}$ (that we called R_H in the RF model), on D_C for different values of the RA: $D_R/J = 0.03, 0.1, 0.3$ in 100×100 and 500×500 systems. When R_{\perp} becomes small compared to the size of the system, its expected $(J/D_C)^{1/2}$ scaling, which is independent of D_R and system size, is confirmed numerically with excellent accuracy. This result provides additional confidence in the conceptual equivalence of the RF and RA models.

III. DYNAMICS

We shall now consider the dynamics of spin excitations close to saturation. As before, we will do it analytically for the RF model first, and then numerically for the CA+RA model. The equivalence of the two models in terms of the dependence of the physical quantities on parameters will be demonstrated again. Our most interesting nontrivial observation is the localization of spin excitations close to saturation where one would have ex-

pected a more conventional uniform ferromagnetic resonance. We shall see that randomness in the directions of small transversal components of the magnetization is still sufficient for localizing excitations.

A. Spin excitations in the RF magnet near saturation: Analytical theory

For a random-field ferromagnet, the Landau-Lifshitz equation reads

$$\hbar \frac{\partial \mathbf{S}}{\partial t} = \mathbf{S} \times \mathbf{H}_{\text{eff}}, \quad (32)$$

where

$$\mathbf{H}_{\text{eff}} = -\frac{\delta \mathcal{H}}{\delta \mathbf{S}} = J \nabla^2 \mathbf{S} + \mathbf{H} + \mathbf{h}, \quad (33)$$

With an eye on excitations we consider $\mathbf{S}(\mathbf{r}) = \mathbf{S}_0(\mathbf{r}) + \boldsymbol{\sigma}(\mathbf{r}, t)$ where $\mathbf{S}_0 = S \hat{z} + \mathbf{s}_{\perp}(\mathbf{r})$ is the equilibrium magnetization and $\boldsymbol{\sigma}(\mathbf{r}, t)$ is the time-dependent perturbation that we choose in the form $\boldsymbol{\sigma}(\mathbf{r}, t) = \boldsymbol{\sigma}(\mathbf{r}) \exp(-i\omega t)$. The linearized equation of motion is

$$\begin{aligned} -i\hbar\omega\boldsymbol{\sigma} &= Ja^{d+2}S\hat{z} \times \nabla^2\boldsymbol{\sigma} + Ja^{d+2}\mathbf{s}_{\perp} \times \nabla^2\boldsymbol{\sigma} \\ &+ Ja^{d+2}\boldsymbol{\sigma} \times \nabla^2\mathbf{s}_{\perp} + \boldsymbol{\sigma} \times \mathbf{H} + \boldsymbol{\sigma} \times \mathbf{h}. \end{aligned} \quad (34)$$

Substituting here

$$Ja^{d+2}\nabla^2\mathbf{s}_{\perp} = Ja^{d+2}k_H^2\mathbf{s}_{\perp} - \mathbf{h}_{\perp} \quad (35)$$

from Eq. (14), we obtain

$$\begin{aligned} -i\hbar\omega\boldsymbol{\sigma} &= Ja^{d+2}S\hat{z} \times \nabla^2\boldsymbol{\sigma} + Ja^{d+2}\mathbf{s}_{\perp} \times \nabla^2\boldsymbol{\sigma} \\ &+ Ja^{d+2}k_H^2\boldsymbol{\sigma} \times \mathbf{s}_{\perp} + H\boldsymbol{\sigma} \times \hat{z} + h_z\boldsymbol{\sigma} \times \hat{z}. \end{aligned} \quad (36)$$

The smallest terms in the right-hand side of the above equation are $Ja^{d+2}\mathbf{s}_{\perp} \times \nabla^2\boldsymbol{\sigma} + Ja^{d+2}k_H^2\boldsymbol{\sigma} \times \mathbf{s}_{\perp} + h_z\boldsymbol{\sigma} \times \hat{z}$. The first two must contribute negligibly to the time-dependent perturbation because close to saturation $\boldsymbol{\sigma}$ is dominated by the x, y components. This allows one to simplify Eq. (40) as

$$-i\hbar\omega\boldsymbol{\sigma} - Ja^{d+2}S\hat{z} \times \nabla^2\boldsymbol{\sigma} - H\boldsymbol{\sigma} \times \hat{z} = h_z\boldsymbol{\sigma} \times \hat{z}. \quad (37)$$

In components one has

$$\begin{aligned} -i\hbar\omega\sigma_x - H\sigma_y + Ja^{d+2}S\nabla^2\sigma_y &= h_z\sigma_y \\ -i\hbar\omega\sigma_y + H\sigma_x - Ja^{d+2}S\nabla^2\sigma_x &= -h_z\sigma_x \end{aligned} \quad (38)$$

Multiplying the first equation by i and subtracting the second equation from it, we obtain

$$Ja^{d+2}S\nabla^2\sigma - (H - \hbar\omega)\sigma = h_z\sigma, \quad (39)$$

where $\sigma \equiv \sigma_x + i\sigma_y$.

Switching to three spatial dimensions, it is convenient to write this last equation in the form

$$\nabla^2\sigma - k_{\omega}^2\sigma = \frac{h_z}{Jsa^2}\sigma, \quad (40)$$

where

$$k_\omega^2 \equiv \frac{H - \hbar\omega}{Jsa^2}. \quad (41)$$

When the small right-hand side of Eq. (40) is neglected, one obtains the spin-wave solution with the wave vector k satisfying $k^2 = k_\omega^2$, that is

$$\hbar\omega = H + Js(ak)^2, \quad (42)$$

as for a conventional ferromagnet. We will see, however, that the static randomness in the right-hand side of Eq. (40) makes such spin waves localized. Using the 3D Green function of that equation, $G(r) = -e^{-k_\omega r}/(4\pi r)$, one can write its formal solution as

$$\sigma(\mathbf{r}) = -\frac{1}{4\pi Jsa^2} \int d^3r' \frac{e^{-k_\omega|\mathbf{r}-\mathbf{r}'|}}{|\mathbf{r}-\mathbf{r}'|} h_z(\mathbf{r}')\sigma(\mathbf{r}'), \quad (43)$$

so that

$$\begin{aligned} \langle |\sigma(\mathbf{r})|^2 \rangle &= \frac{1}{16\pi^2 J^2 s^2 a^4} \int d^3r' \int d^3r'' \times \\ &\frac{e^{-k_\omega|\mathbf{r}-\mathbf{r}'|} e^{-k_\omega|\mathbf{r}-\mathbf{r}''|}}{|\mathbf{r}-\mathbf{r}'||\mathbf{r}-\mathbf{r}''|} \langle h_z(\mathbf{r}')h_z(\mathbf{r}'')\sigma(\mathbf{r}')\sigma^*(\mathbf{r}'') \rangle. \end{aligned} \quad (44)$$

For long-wavelength oscillations, assuming that $\sigma(\mathbf{r})$ is correlated on a scale that is much greater than the atomic scale on which $h_z(\mathbf{r})$ is correlated, the average under the integral factorizes:

$$\begin{aligned} \langle h_z(\mathbf{r}')h_z(\mathbf{r}'')\sigma(\mathbf{r}')\sigma^*(\mathbf{r}'') \rangle &= \langle h_z(\mathbf{r}')h_z(\mathbf{r}'') \rangle \langle \sigma(\mathbf{r}')\sigma^*(\mathbf{r}'') \rangle \\ &= \frac{1}{3} h^2 a^3 \delta(\mathbf{r}' - \mathbf{r}'') \langle \sigma(\mathbf{r}')\sigma^*(\mathbf{r}'') \rangle. \end{aligned} \quad (45)$$

This gives

$$\begin{aligned} \langle |\sigma(\mathbf{r})|^2 \rangle &= \frac{h^2}{48\pi^2 J^2 s^2 a^4} \int d^3r' \frac{e^{-2k_\omega|\mathbf{r}-\mathbf{r}'|}}{|\mathbf{r}-\mathbf{r}'|^2} \langle |\sigma(\mathbf{r}')|^2 \rangle \\ &= \frac{1}{4\pi R_f} \int d^3r' \frac{e^{-2k_\omega|\mathbf{r}-\mathbf{r}'|}}{|\mathbf{r}-\mathbf{r}'|^2} \langle |\sigma(\mathbf{r}')|^2 \rangle, \end{aligned} \quad (46)$$

where we have used Eq. (7) for R_f in 3D: $R_f = 12\pi(Js/h)^2 a$. Eq. (46) is satisfied if

$$1 = \frac{1}{4\pi R_f} \int d^3r' \frac{e^{-2k_\omega|\mathbf{r}-\mathbf{r}'|}}{|\mathbf{r}-\mathbf{r}'|^2} = \frac{2}{k_\omega R_f}, \quad (47)$$

which gives $k_\omega = 2/R_f$. With account of Eq. (18), one obtains

$$k_\omega^2 = \frac{H - \hbar\omega}{Jsa^2} = \frac{4}{R_f^2}, \quad \hbar\omega = H \left[1 - \left(\frac{2R_H}{R_f} \right)^2 \right], \quad (48)$$

which is slightly below the FMR frequency due to the disorder and due to the condition $R_H \ll R_f$ corresponding to the field range close to saturation.

An easy check of the self-consistency of the above result comes from the following consideration based on the

conceptual equivalence of the RF and RA models. As would be expected from the results of Ref. 43, tested numerically, at $H = 0$ the FMR frequency should be determined by the fluctuation of \mathbf{h} on the scale R_f : $\hbar\omega \sim h(a/R_f)^{3/2} \propto h(h/Js)^3$. We now observe that as H becomes small in Eq. (48), and $(2R_H/R_f)^2$ becomes of order unity, the frequency of the oscillations, as expected, becomes $\hbar\omega \sim H(R_H/R_f)^2 \propto h^4/(Js)^3$. It is interesting to notice that a small correction Δ to the FMR frequency $\omega_{FMR} = H$, which makes the resonance frequency equal $\omega = H - \Delta$, is independent of H . One has $\Delta \sim h^2/J$ in 2D, and $\Delta \sim h^4/J^3$ in 3D.

Switching to two spatial dimensions, the use of the 2D Green function, $G(r) = K_0(k_\omega r)/(2\pi)$, modifies the equations as follows

$$\sigma(\mathbf{r}) = \frac{1}{2\pi Jsa^2} \int d^2r' K_0[k_\omega|\mathbf{r}-\mathbf{r}'|] h_z(\mathbf{r}')\sigma(\mathbf{r}'), \quad (49)$$

$$\begin{aligned} \langle |\sigma(\mathbf{r})|^2 \rangle &= \frac{1}{4\pi^2 J^2 s^2 a^4} \int d^2r' \int d^2r'' \times \\ &K_0[k_\omega|\mathbf{r}-\mathbf{r}'|] K_0[k_\omega|\mathbf{r}-\mathbf{r}''|] \langle h_z(\mathbf{r}')h_z(\mathbf{r}'')\sigma(\mathbf{r}')\sigma^*(\mathbf{r}'') \rangle. \end{aligned} \quad (50)$$

With

$$\langle h_z(\mathbf{r}')h_z(\mathbf{r}'')\sigma(\mathbf{r}')\sigma^*(\mathbf{r}'') \rangle = \langle h_z(\mathbf{r}')h_z(\mathbf{r}'') \rangle \langle \sigma(\mathbf{r}')\sigma^*(\mathbf{r}'') \rangle \quad (51)$$

and

$$\langle h_z(\mathbf{r}')h_z(\mathbf{r}'') \rangle = \frac{1}{3} \langle h^2 \rangle a^2 \delta(\mathbf{r}' - \mathbf{r}'') \quad (52)$$

this gives for the three-component spin field and three-component random field

$$\begin{aligned} \langle |\sigma(\mathbf{r})|^2 \rangle &= \frac{h^2}{12\pi^2 J^2 s^2 a^4} \int d^2r' K_0^2[k_\omega|\mathbf{r}-\mathbf{r}'|] \langle |\sigma(\mathbf{r}')|^2 \rangle \\ &\sim \frac{1}{(R_f k_\omega)^2} \langle |\sigma(\mathbf{r}')|^2 \rangle, \end{aligned} \quad (53)$$

where we have used $R_f/a \sim Js/h$ in 2D. This again gives $k_\omega = 1/R_f$ and $1 - \hbar\omega/H \sim (R_H/R_f)^2$. Thus, in all dimensions $R_\omega = 1/k_\omega$ is independent of the frequency and is of the order of R_f which is the ferromagnetic correlation length at $H = 0$.

For spin excitations of frequency ω in 3D

$$\begin{aligned} \langle \sigma(\mathbf{r}_1) \cdot \sigma(\mathbf{r}_2) \rangle &= \frac{1}{16\pi^2 J^2 s^2 a^4} \int d^3r' \int d^3r'' \times \\ &\frac{e^{-k_\omega|\mathbf{r}_1-\mathbf{r}'|} e^{-k_\omega|\mathbf{r}_2-\mathbf{r}''|}}{|\mathbf{r}_1-\mathbf{r}'||\mathbf{r}_2-\mathbf{r}''|} \langle h_z(\mathbf{r}')h_z(\mathbf{r}'')\sigma(\mathbf{r}')\sigma^*(\mathbf{r}'') \rangle \\ &= \frac{\langle |\sigma|^2 \rangle}{4\pi R_f} \int d^3r \frac{e^{-k_\omega|\mathbf{r}_1-\mathbf{r}|}}{|\mathbf{r}_1-\mathbf{r}|^2} \frac{e^{-k_\omega|\mathbf{r}_2-\mathbf{r}|}}{|\mathbf{r}_2-\mathbf{r}|^2} = \langle |\sigma|^2 \rangle e^{-k_\omega|\mathbf{r}_1-\mathbf{r}_2|}. \end{aligned} \quad (54)$$

In 2D one obtains

$$\langle \sigma(\mathbf{r}_1) \cdot \sigma(\mathbf{r}_2) \rangle = \langle |\sigma|^2 \rangle k_\omega |\mathbf{r}_1 - \mathbf{r}_2| K_1(k_\omega |\mathbf{r}_1 - \mathbf{r}_2|). \quad (55)$$

This suggests that in the field range corresponding to $a \ll R_H \ll R_f$, spin excitations are localized on the

scale $R_\omega = 1/k_\omega \sim R_f \gg R_H$ independently of the frequency and the magnetic field. Such independence of the localization length on the frequency has been seen in our previous numerical studies of localization [44].

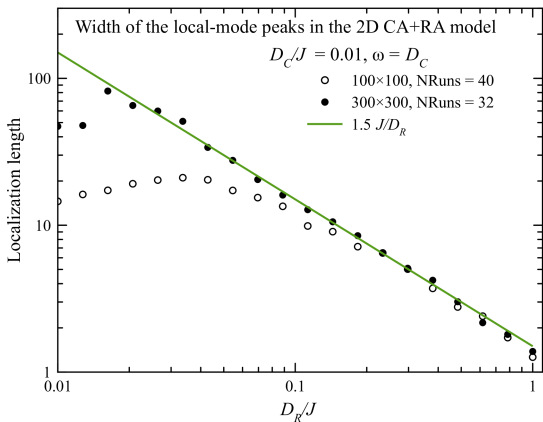
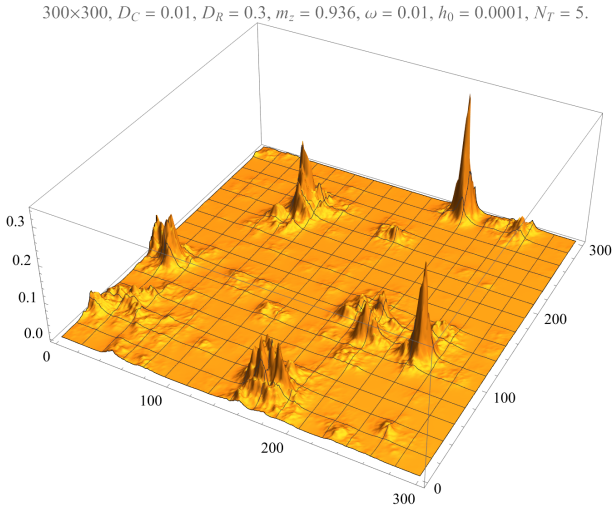


Figure 4. Upper panel: Localization of spin excitations in a 2D RA model with coherent anisotropy. Lower panel: Dependence of the localization length on the RA scales as J/D_R in accordance with theoretical prediction as soon as the peak width becomes small compared to the size of the system.

B. Spin excitations in the RA magnet with coherent anisotropy: Numerical experiment

Close to saturation, the ferromagnetic resonance in the CA+RA model is located at $\hbar\omega = D_C$. Numerical analysis of the oscillations of the magnetization at that frequency shows a pronounced spatial localization of spin excitations, see the upper panel in Fig. 4. Here, starting from the equilibrium state \mathbf{s}_0 at $T = 0$ found by the energy minimization starting from the collinear spin state along z axis, the system was excited by the uniform magnetic field of a small amplitude polarized perpendicularly to z axis. The undamped Landau-Lifshitz equation

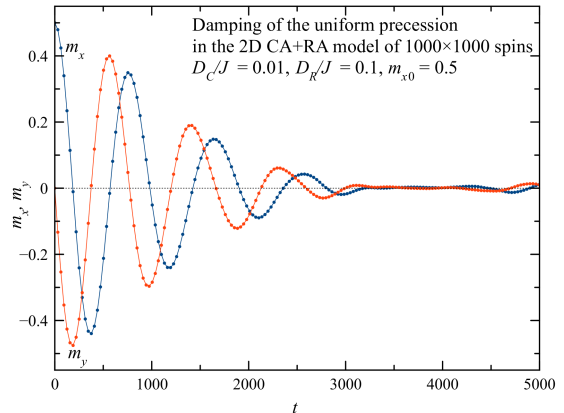


Figure 5. Damping of the uniform precession of the magnetization. Time dependence of m_x and m_y for a large initial deviation, $m_{x0} = 0.5$.

of motion for classical spins was solved with the help of the 5th-order Runge-Kutta Butcher's method, and the square of the spin deviation $(\mathbf{s} - \mathbf{s}_0)^2$ was plotted after several periods of the pumping. The localization length was computed as the average width of the local-mode peaks such as in the upper panel in Fig. 4. To compute this width, we used the mn method (see around Eq. 30 of Ref. [44]). Previously, we have demonstrated numerically [43, 44] the localization of spin excitations in a pure RA model with $D_C = 0$, which must be expected in the random medium. The spatial localization of the FMR oscillations has been observed in experiments [39–42] both away from and close to saturation. In the latter case, however, when all spins are almost aligned, it is less obvious from the theoretical perspective.

As is shown in the lower panel of Fig. 4, the localization length for spin excitations decreases on increasing D_R as J/D_R . This agrees perfectly with the analytical result of the previous section that the localization length is determined by the ferromagnetic length at $D_C = 0$ that scales as J/D_R in 2D.

C. Decay of the uniform precession due to RA

As excitation modes of the magnet are spatially localized in the presence of RA, the uniform precession is not a mode of the system and it is decaying into the local modes. Our numerical analysis shows that in the presence of RA the uniform precession is damped. Its decay at $T = 0$ after the magnetization $\mathbf{m} = (1/N) \sum_i \mathbf{s}_i$ of a collinear state was directed at an angle with respect to z axis is shown in Figs. 5 and 6. Here, again, we solved the undamped Landau-Lifshitz equation of motion for classical spins with the help of the 5th-order Runge-Kutta Butcher's method. At $D_R = 0$ there is an undamped uniform precession around z axis. However, as soon as

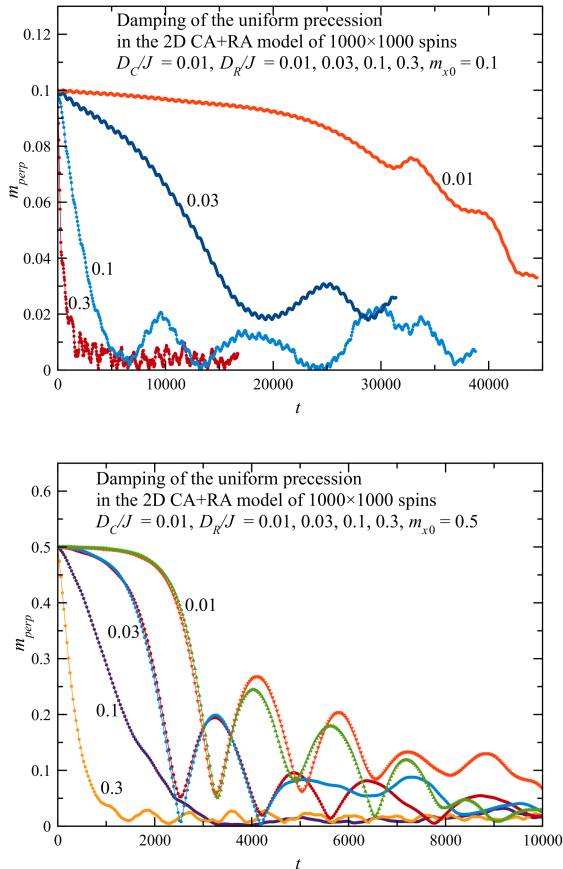


Figure 6. Time dependence of the perpendicular component of the magnetization for three values of the RA. Upper panel: small initial deviation, $m_{x0} = 0.1$. Lower panel: large initial deviation, $m_{x0} = 0.5$.

the RA is turned on, uniform precession decays. As can be seen from in Fig. 6, the effect increases with increasing the RA strength. For small D_R and large initial deviation from z axis, $m_{x0} = 0.5$, the decay is strongly nonlinear and shows partial recurrence.

The oscillating dynamics in the CA+RA model leads to ferromagnetic-resonance absorption peak near the frequency defined by the core anisotropy, $\omega \simeq D_C/\hbar$, unlike the broadband absorption in the RA model. The peak is shifted to the left, however, due to the effect of the temperature and RA, the latter in accordance with Eq. (48). The RA and nonzero temperature also contribute to the width of the microwave absorption peak. Even for $D_R = 0$, finite temperature provides the frequency shift and finite line width due to the spin-wave scattering.

IV. CONCLUSIONS

We have studied disordered ferromagnets within random-field and random-anisotropy models that include

the external field and coherent anisotropy. The latter, even when they are weak compared to their random counterparts, bring the magnet close to saturation. This is a well-known property of amorphous ferromagnets which exhibit record low coercive field and record high magnetic susceptibility. Consequently, for sufficiently small disordered ferromagnets that do not break into conventional magnetic domains, the vicinity of saturation is the most interesting regime of practical importance.

The dependence of the spin-spin correlation function on the parameters of the model has been computed in this regime for a three-component spin in two (thin film) and three (bulk material) dimensions. Good agreement between analytical and numerical results has been obtained. In the absence of the saturating force (that is, without the external field H or coherent anisotropy D_C), the ferromagnetic correlation length scales inversely as the first power of the disorder strength in 2D and as the second power in 3D. Close to saturation, the transversal spin-spin correlations are of interest. We have shown that they decay exponentially, with the correlation length that scales as $1/\sqrt{H}$ in the random field model with the external field H , and as $1/\sqrt{D_C}$ in the random anisotropy model with the coherent anisotropy D_C .

Turning to spin excitations, we have demonstrated that in the vicinity of the ferromagnetic resonance they are localized regardless of how close to saturation the system is. Somewhat counterintuitive is the fact that the localization length is determined by the strength of the disorder and not by the correlation length of the transverse spin-spin correlations. This result has been obtained analytically and confirmed numerically. The disorder is also responsible for the damping of spin oscillations, which goes up on increasing the disorder strength.

ACKNOWLEDGEMENT

This work has been supported by Grant No. FA9550-24-1-0090 funded by the Air Force Office of Scientific Research.

DATA AVAILABILITY STATEMENT

Generated numerical data is available upon reasonable request.

AUTHOR CONTRIBUTION STATEMENT

The authors contributed equally to the work.

-
- [1] E.M. Chudnovsky and R.A. Serota, Spin-glass and ferromagnetic states in amorphous solids, *Physical Review B* **26**, 2697-2699 (1982).
- [2] E. M. Chudnovsky, A theory of two-dimensional amorphous ferromagnet, *Journal of Magnetism and Magnetic Materials* **40**, 21-16 (1983).
- [3] A. Aharony and E. Pytte, Low-temperature scaling for systems with random fields and anisotropies, *Physical Review B* **27**, 5872-5874 (1983).
- [4] E. M. Chudnovsky, W. M. Saslow, and R. A. Serota, Ordering in ferromagnets with random anisotropy, *Physical Review B* **33**, 251-261 (1986).
- [5] E. M. Chudnovsky, Random Anisotropy in Amorphous Alloys, Chapter 3 in the Book: *Magnetism of Amorphous Metals and Alloys*, edited by J. A. Fernandez-Baca and W.-Y. Ching, pages 143-174 (World Scientific, Singapore, 1995).
- [6] R. Fisch, Power-law correlations and orientational glass in random-field Heisenberg models, *Physical Review B* **57**, 269-278 (1998).
- [7] R. Fisch, Random field and random anisotropy effects in defect-free three-dimensional XY models, *Physical Review B* **62**, 361-366 (2000).
- [8] E. M. Chudnovsky and J. Tejada, *Lectures on Magnetism* (Rinton Press, Princeton, New Jersey, 2006).
- [9] R. Fisch, Structure factor of the three-dimensional random-field XY model: Monte Carlo calculations, *Physical Review B* **76**, 214435-(5) (2007).
- [10] D. A. Garanin, E. M. Chudnovsky, and T. Proctor, Random field xy model in three dimensions, *Physical Review B* **88**, 224418-(21) (2013).
- [11] T. C. Proctor, D. A. Garanin, and E. M. Chudnovsky, Random fields, Topology, and Imry-Ma argument, *Physical Review Letters* **112**, 097201-(4) (2014).
- [12] D. A. Garanin and E. M. Chudnovsky, Ordered vs. disordered states of the random-field model in three dimensions, *European Physics Journal B* **88**, 81-(19) (2015).
- [13] T. C. Proctor, E. M. Chudnovsky, and D. A. Garanin, Scaling of coercivity in a 3d random anisotropy model, *Journal of Magnetism and Magnetic Materials*, **384**, 181-185 (2015).
- [14] E. M. Chudnovsky and D. A. Garanin, Topological order generated by a random field in a 2D exchange model, *Physical Review Letters* **121**, 017201-(4) (2018).
- [15] D. A. Garanin and E. M. Chudnovsky, Random anisotropy magnet at finite temperature, *Journal of Physics: Condensed Matter* **34**, 285801-(15) (2022).
- [16] Y. Imry and S.-k. Ma, Random-field instability of the ordered state of continuous symmetry, *Physical Review Letters* **35**, 1399-1401 (1975).
- [17] W. M. Saslow and C. Sun, Longitudinal resonance for thin film ferromagnets with random anisotropy, *Physical Review B* **98**, 214415-(6) (2018).
- [18] P. Monod and Y. Berthier, Zero field electron spin resonance of Mn in the spin glass state, *Journal of Magnetism and Magnetic Materials* **15-18**, 149-150 (1980).
- [19] J. J. Prejean, M. Joliclerc, and P. Monod, Hysteresis in CuMn: The effect of spin orbit scattering on the anisotropy in the spin glass state, *Journal de Physique (Paris)* **41**, 427-435 (1980).
- [20] H. Alloul and F. Hippert, Macroscopic magnetic anisotropy in spin glasses: transverse susceptibility and zero field NMR enhancement, *Journal de Physique Lettres* **41**, L201-204 (1980).
- [21] S. Schultz, E. M. Gulliksen, D. R. Fredkin, and M. Tovar, Simultaneous ESR and magnetization measurements characterizing the spin-glass state, *Physical Review Letters* **45**, 1508-1512 (1980).
- [22] E. M. Gullikson, D. R. Fredkin, and S. Schultz, Experimental demonstration of the existence and subsequent breakdown of triad dynamics in the spin-glass CuMn, *Physical Review Letters* **50**, 537-540 (1983).
- [23] E. Sheftel, E. Harin, V. Tredzhetov, and Y. Koksharov, Ferromagnetic resonance and random magnetic anisotropy in nanocrystalline Fe-Zr-N films, *European Physics Journal* **185**, 04004-(4) (2018).
- [24] A. Fert and P. M. Levy, Role of anisotropic exchange interactions in determining the properties of spin-glasses, *Physical Review Letters* **44**, 1538-1541 (1980).
- [25] P. M. Levy and A. Fert, Anisotropy induced by non-magnetic impurities in CuMn spin-glass alloys, *Physical Review B* **23**, 4667 (1981).
- [26] C. L. Henley, H. Sompolinsky, and B. I. Halperin, Spin-resonance frequencies in spin-glasses with random anisotropies, *Physical Review B* **25**, 5849-5855, (1982).
- [27] B. I. Halperin and W. M. Saslow, Hydrodynamic theory of spin waves in spin glasses and other systems with non-collinear spin orientations, *Physical Review B* **16**, 2154-2162 (1977).
- [28] W. M. Saslow, Anisotropy-triad dynamics, *Physical Review Letters* **48**, 505-508 (1982).
- [29] R. Bruinsma and S. N. Coppersmith, Anderson localization and breakdown of hydrodynamics in random ferromagnets, *Physical Review B* **33**, 6541-6544(R) (1986).
- [30] R. A. Serota, Spin-wave localization in ferromagnets with weak random anisotropy, *Physical Review B* **37**, 9901-9903(R) (1988).
- [31] M. Ma, B. I. Halperin, and P.A. Lee, Strongly disordered superfluids: Quantum fluctuations and critical behavior, *Physical Review B* **34**, 3136-3143 (1986).
- [32] L. Zhang, Disordered boson systems: A perturbative study, *Physical Review B* **47**, 14364-14373 (1993).
- [33] J. P. Álvarez Zúñiga and N. Laflorencie, Bose-glass transition and spin-wave localization for 2D bosons in a random potential, *Physical Review Letters* **111**, 160403-(5) (2013).
- [34] X. Yu and M. Müller, Localization of disordered bosons and magnets in random fields, *Annals of Physics* **337**, 55-93 (2013).
- [35] M. Evers, C. A. Müller, and U. Nowak, Spin-wave localization in disordered magnets, *Physical Review B* **92**, 014411 (2015).
- [36] V. S. Amaral, B. Barbara, J. B. Sousa, and J. Filippi, Spin-wave localization in random anisotropy systems: Amorphous $(Dy_xGd_{1-x})Ni$, *European Physics Letters* **22** 139-144 (1993).
- [37] S. Suran and E. Boumaiz, Longitudinal resonance in ferromagnets with random anisotropy: A formal experimental demonstration, *Journal of Applied Physics* **81**, 4060 (1997).

- [38] G. Suran, Z. Frait, and E. Boumaz, Direct observation of the longitudinal resonance mode in ferromagnets with random anisotropy, *Physical Review B* **55**, 11076-11079 (1997).
- [39] S. Suran and E. Boumaiz, Longitudinal-transverse resonance and localization related to the random anisotropy in a-CoTbZr films, *Journal of Applied Physics* **83**, 6679 (1998).
- [40] R. D. McMichael, D. J. Twisselmann, and A. Kunz, Localized ferromagnetic resonance in inhomogeneous thin film, *Physical Review Letters* **90**, 227601-(4) (2003).
- [41] G. de Loubens, V. V. Naletov, O. Klein, J. Ben Youssef, F. Boust, and N. Vukadinovic, Magnetic resonance studies of the fundamental spin-wave modes in individual sub-micron Cu/NiFe/Cu perpendicularly magnetized disks, *Physical Review Letters* **98**, 127601-(4) (2007).
- [42] C. Du, R. Adur, H. Wang, S. A. Manuilov, F. Yang, D. V. Pelekhov, and P. C. Hammel, Experimental and numerical understanding of localized spin wave mode behavior in broadly tunable spatially complex magnetic configurations, *Physical Review B* **90**, 214428-(10) (2014).
- [43] D. A. Garanin and E. M. Chudnovsky, Absorption of microwaves by random-anisotropy magnets, *Physical Review B* **103**, 214414-(11) (2021).
- [44] D. A. Garanin and E. M. Chudnovsky, Localized spin-wave modes and microwave absorption in random-anisotropy ferromagnets, *Physical Review B* **107**, 134411-(13)(2023).
- [45] D. A. Garanin and E. M. Chudnovsky, Nonlinear and thermal effects in the absorption of microwaves by random anisotropy magnets, *Physical Review B* **105**, 064402-(8) (2022).
- [46] E. M. Chudnovsky and D. A. Garanin, Integral absorption of microwave power by random-anisotropy magnets, *Physical Review B* **107**, 224413-(9) (2023).
- [47] E. M. Chudnovsky and D. A. Garanin, Scaling theory of magnetic order and microwave absorption in amorphous and granular ferromagnets, *Physical Review B* **109**, 054429-(10) (2024).
- [48] D. A. Garanin and E. M. Chudnovsky, Scaling of static and dynamical properties of random anisotropy magnets, *Europhysics Letters* **148**, 26001-(6) (2024).
- [49] X. Zeng, X. Cheng, R. Yu, and G. D. Stucky, Electromagnetic microwave absorption theory and recent achievements in microwave absorbers, *Carbon* **168**, 606-623 (2020).
- [50] H. S. M. Al'Azzavi, A. B. Granovskii, Yu. E. Kalinin, V. A. Makagonov, A. V. Sitnikov, and O. S. Tarasova, Influence of oxidized interlayers on magnetic properties of multilayer films based on amorphous ferromagnet - dielectric nanocomposites, *Physics of the Solid State* **58**, 938-945 (2016).
- [51] P. Martin and A. Hernando, Applications of amorphous and nanocrystalline magnetic materials, *Journal of Magnetism and Magnetic Materials* **215-216**, 729-734 (2000).
- [52] J. V. I. Jaakko et al., Magnetic nanocomposites at microwave frequencies, in a book: *Trends in Nanophysics*, edited by V. Barsan and A. Aldea, pages 257-285 (Springer, New York, 2010).
- [53] J. Calvo-de la Rosa, A. Bou-Comas, J. M. Hernández, P. Marín, J. S. Lopez-Villegas, J. Tejada, and E. M. Chudnovsky, New approach to designing functional materials for stealth technology: Radar experiment with bilayer absorbers and optimization of the reflection loss, *Advanced Functional Materials* **2023**, 2308819-(8) (2023).